

RESEARCH

Open Access



# Diverse effects of coronavirus-defective viral genomes on the synthesis of IFN $\beta$ and ISG15 mRNAs and coronavirus replication

Hsuan-Wei Hsu<sup>1</sup>, Li-Kang Chang<sup>1</sup>, Chun-Chun Yang<sup>1</sup>, Ching-Hung Lin<sup>2</sup>, Yu Teng<sup>1</sup>, Pei-Chi Hsu<sup>1</sup>, Cheng-Yao Yang<sup>1</sup> and Hung-Yi Wu<sup>1\*</sup>

## Abstract

**Background** The mechanism by which coronavirus-defective viral genomes (DVGs) affect coronavirus and host cells during infection remains unclear. A variety of DVGs with different RNA structures can be synthesized from coronavirus-infected cells, and these DVGs can also encode proteins. Consequently, in the present study, we first dissected the effects of individual DVGs on the synthesis of IFN $\beta$  and ISG15 mRNAs at the RNA, protein and combined levels, and then examined whether different coronavirus-DVGs have different effects on the synthesis of IFN $\beta$  and ISG15 mRNAs and coronavirus replication both individually and collectively under different infection conditions.

**Methods** To dissect the effects of individual DVGs on the synthesis of IFN $\beta$  and ISG15 mRNAs at the RNA, protein and combined levels, DVG 2.2 and DVG 5.1, which were previously identified in coronavirus-infected cells, and their mutants were constructed followed by transfection. Western blot and RT–qPCR were used to detect the synthesis of protein and to quantify the synthesis of IFN $\beta$  and ISG15 mRNAs, respectively. To examine whether different coronavirus-DVGs have different effects on the synthesis of IFN $\beta$  and ISG15 mRNAs and coronavirus replication both individually and collectively under different infection conditions, different naturally occurring DVGs were selected and constructed followed by transfection after or before coronavirus infection and by RT–qPCR and hemagglutination assay.

**Results** These results suggested that (i) coronavirus-DVGs at the RNA, protein and combined levels have different effects on the synthesis of IFN $\beta$  and ISG15 mRNAs, (ii) coronavirus-DVGs can inhibit coronavirus replication at least partly through interferon signaling and (iii) different DVGs have different effects on the synthesis of IFN $\beta$  and ISG15 mRNAs and coronavirus replication both individually and collectively under different infection conditions.

**Conclusions** Coronavirus replication can be regulated by diverse coronavirus-derived DVGs at least partly through innate immunity. Such regulation may contribute to the pathogenesis of coronavirus. The DVG populations in coronavirus-infected cells with the ability to inhibit coronavirus replication are expected to be potential resources for the identification of antivirals at the level of RNA, protein or in combination, and the methods used in the current study can be used as a platform for this purpose.

\*Correspondence:  
Hung-Yi Wu  
hwu2@dragon.nchu.edu.tw

<sup>1</sup>Graduate Institute of Veterinary Pathobiology, College of Veterinary Medicine, National Chung Hsing University, Taichung 40227, Taiwan  
<sup>2</sup>Department of Veterinary Medicine, National Pingtung University of Science and Technology, Neipu, Pingtung 91201, Taiwan



© The Author(s) 2025. **Open Access** This article is licensed under a Creative Commons Attribution-NonCommercial-NoDerivatives 4.0 International License, which permits any non-commercial use, sharing, distribution and reproduction in any medium or format, as long as you give appropriate credit to the original author(s) and the source, provide a link to the Creative Commons licence, and indicate if you modified the licensed material. You do not have permission under this licence to share adapted material derived from this article or parts of it. The images or other third party material in this article are included in the article's Creative Commons licence, unless indicated otherwise in a credit line to the material. If material is not included in the article's Creative Commons licence and your intended use is not permitted by statutory regulation or exceeds the permitted use, you will need to obtain permission directly from the copyright holder. To view a copy of this licence, visit <http://creativecommons.org/licenses/by-nc-nd/4.0/>.

## Background

Coronaviruses (CoVs), which belong to the family *Coronaviridae*, order *Nidovirales*, contain the largest known viral RNA genome (~30 kilobases) [1, 2]. CoVs are important pathogens both in humans and animals and have caused widespread and costly diseases, such as COVID-19 caused by severe acute respiratory syndrome coronavirus 2 (SARS-CoV-2) [3–6]. In addition to genomic RNA, the synthesis of a nested set of subgenomic mRNAs (sgmRNAs) is a feature of *Nidovirales*. Other coronavirus transcripts, including defective viral genomes (DVGs), have also been identified in coronavirus-infected cells via next-generation sequencing [7–9].

DVGs are byproducts derived from their parental viral genomes and have been identified in most RNA viruses [10]. DVGs are speculated to be synthesized through a copy-choice template-switching recombination process, resulting in a variety of genome structures with mutations, truncations or rearrangements [11]. The deletion type of DVGs or double-stranded RNA intermediates generated during the replication of DVGs can also induce the expression of interferon (IFN) and IFN-stimulated genes (ISGs) through the activation of pattern recognition receptors and IFN pathways [12–14]. Characterization of coronavirus DVGs suggests that DVGs are reproducible overall under regular infection, but the species and amounts of DVGs are altered under different infection environments and selection pressures [8]. These characteristics of DVGs may suggest their important roles in the pathogenesis of RNA viruses.

Recognition of viral RNA structures by the cytosolic RNA helicases melanoma differentiation-associated gene 5 (MDA5) and retinoic acid-inducible gene 1 (RIG-I) can lead to the activation of downstream transcription factors, including IRF3, IRF7, AP-1 and NF- $\kappa$ B, and then to initiate the gene expression of IFN [15, 16]. RIG-I is responsible for the recognition of uncapped 5' triphosphates on viral RNA [17, 18], and MDA5 can detect secondary or tertiary RNA structures and double-stranded RNA motifs [19–22]. The expressed IFN can bind to the IFN receptor to activate JAK1, TYK2 and downstream STAT transcription factors, inducing the expression of IFN-stimulated genes (ISGs) and limiting viral replication [23, 24]. In terms of virus–host interactions, innate immunity can be activated in coronavirus-infected cells, and coronavirus proteins can inhibit the IFN signaling pathway through interactions with IFN signaling-related proteins to counteract host defenses, ensuring efficient coronavirus replication [25].

Studies on the mechanism by which coronavirus DVG affects coronavirus and host cells during infection are still limited. Previous studies have shown that the number of DVGs derived from SARS-CoV-2 is correlated with the level of host IFN response and the stage

of disease development [26]. Although it has been suggested that the DVG species vary under different infection conditions [8], whether different DVG species can lead to different virus–host interactions under different infection environments remains to be clarified. In addition, another study suggested that the protein expressed from a SARS-CoV-2 DVG species identified after 20 virus passages can attenuate virus replication [27]. However, in addition to the DVG-encoded proteins, whether DVGs can attenuate virus replication at the level of RNA or at the level of both the RNA and protein also remains to be determined.

Accordingly, in contrast to previous studies, in the present study, we investigated the effects of individual DVGs on the synthesis of IFN signaling-related mRNAs at the RNA, protein and combined levels, and found that DVGs at the RNA, protein or combined levels have different effects the synthesis of IFN $\beta$  and ISG15 mRNAs. It is important to dissect the function of DVGs at the levels of RNA, protein, and both because the identified functions may have the potential to be antivirals if they have the ability to inhibit coronavirus replication. In addition, we also examined whether different DVGs have different effects on the synthesis of IFN $\beta$  and ISG15 mRNAs and coronavirus replication both individually and collectively under different infection conditions. The identified effects of coronavirus DVGs on the synthesis of IFN $\beta$  and ISG15 mRNAs and coronavirus replication may advance our understanding of coronavirus pathogenesis. Coronavirus–DVGs with the ability to inhibit coronavirus replication are expected to be potential resources for the identification of antivirals at the level of RNA, protein or in combination.

## Methods

### Virus and cells

The Mebus strain of bovine coronavirus (BCoV) (GenBank: U00735.2) obtained from David A. Brian (University of Tennessee, TN) and human embryonic kidney 293T (HEK-293T) cells were used in this study. HEK-293 cells were grown in Dulbecco's modified Eagle's medium (DMEM) supplemented with 10% fetal bovine serum at 37 °C with 5% CO<sub>2</sub>.

### Construction of naturally occurring DVGs and in vitro transcription

The DVGs used in the present study were constructed according to the previously identified naturally occurring BCoV DVGs via RT-PCR and nanopore direct RNA sequencing [8, 28, 29] and were subsequently cloned and inserted into plasmids. In brief, 10  $\mu$ g of RNA collected from BCoV-infected cells at 24 hours post infection (hpi) was subjected to reverse transcription (RT) via SuperScript III reverse transcriptase (Thermo Fisher Scientific,

Waltham, USA) according to the manufacturer's instructions. For the construction of DVG species with 5' and 3' UTRs, the resulting cDNA was then used for the identification of DVG species via PCR using AccuPrime DNA polymerases (Thermo Fisher Scientific, Waltham, USA) with primers L20(-) and the corresponding reverse primer (Table S1). To construct DVG species with no 5', 3' or both UTRs, primers were designed (Table S1) on the basis of previous results of nanopore direct RNA sequencing [8, 28]. Overlapping PCR was performed with AccuPrime DNA polymerases (Thermo Fisher Scientific, Waltham, USA). For DVG constructs 5.1 and 2.2 with the introduction of a stop codon ( $\Delta$ DVG 5.1 and  $\Delta$ DVG 2.2, respectively), overlapping PCR was also employed with the respective primers (Table S1). The resulting PCR products were subsequently cloned and inserted into the pCR-XL-2-TOPO vector (Thermo Fisher Scientific, Waltham, USA). To prepare DVG transcripts in vitro, the constructed DVG plasmids were used as templates for amplification by PCR with forward primer T7 (-) and the corresponding reverse primer (Table S1). The PCR products were precipitated and then in vitro-transcribed into RNA transcripts using mMESSAGE mMACHINE™ T7 Transcription Kit (Thermo Fisher Scientific, Waltham, USA).

#### Transfection of DVG transcripts into HEK-293T cells

The in vitro-transcribed DVG transcripts were used in 35-mm-diameter dishes at a concentration of 2000 ng (for the transfection of DVGs individually) or 100 ng per DVG (for the transfection of DVGs collectively) via the Lipofectamine™ 2000 reagent (Thermo Fisher Scientific, Waltham, USA) according to the manufacturer's transfection protocol. Consequently, HEK-293T cells at 70~80% confluency in 35-mm-diameter dishes were infected with BCoV at an MOI of 10 before or after the transfection of DVGs. The total cellular RNA was collected at the desired time points according to the experimental design, as illustrated in each figure. Total cellular RNA was extracted with TRI Reagent™ (Molecular Research Center, Cincinnati, USA) for RT-qPCR, and the cell lysates were collected with Triton X-100 lysis buffer for Western blot.

#### Western blot

To detect the DVG-encoded proteins, cell lysates were prepared from cells treated with Triton X-100 lysis buffer, and the concentrations of the collected cell lysates were quantified via the Bradford protein assay [30]. Equal amounts of cell lysates were subjected to electrophoresis with a 10% SDS polyacrylamide gel for the separation of proteins. After electrophoresis, the proteins in the gel were transferred to polyvinylidene difluoride (PVDF) membranes. Primary antibodies against proteins encoded

by DVG 2.2 and DVG 5.1 and  $\beta$ -actin were added and then incubated at 4 °C for 16 h. Finally, secondary antibodies against the corresponding primary antibodies were incubated at 25 °C for one hour. To detect the target proteins, enhanced chemiluminescence (ECL) was employed, followed by exposure to Kodak XAR-5 film (Kodak, Rochester, NY, USA) for imaging.

#### RT-qPCR

To quantify the DVGs, genomic RNA of BCoV and the cellular mRNAs of IFN $\beta$  and ISG15, the extracted total cellular RNA was reverse transcribed via random hexamers and SuperScript III Reverse Transcriptase (Thermo Fisher Scientific, Waltham, USA). The synthesized cDNA was then used for qPCR with SYBR® Green amplification mix (Roche Applied Science, Mannheim, Germany) according to the manufacturer's protocol. The primer for the detection of DVGs, genomic RNA of BCoV and the cellular mRNAs of IFN $\beta$  and ISG15 are listed in Table S1. Note that the primers used for detecting genomic RNA of BCoV cannot bind to the DVGs selected in the present study. Plasmids containing the same genes encoding DVGs, viral RNA or the cellular mRNAs IFN $\beta$  and ISG15 were diluted ( $10^9$  to  $10^2$  copies per plasmid) and run in parallel with the quantitated cDNA for use in a standard plot. In addition, to compare the effects of diverse DVGs on the synthesis of IFN $\beta$  and ISG15 mRNAs and coronavirus RNA on the same basis, the amounts of IFN $\beta$  and ISG15 mRNAs and coronavirus RNA were normalized to the amounts of individual DVGs. The amounts of quantitated individual DVGs are illustrated in Figs. S1–S6.

#### Hemagglutination (HA) assay

Serial twofold dilutions of the supernatant collected from DVG-transfected HEK-293T cells infected with BCoV were prepared in 50  $\mu$ L amounts in a 96-well V-bottom microtiter plate. An equal volume (50  $\mu$ L) of mouse erythrocytes (1% v/v) in PBS was added to each well, with PBS used as a negative control. The mixtures were incubated at 25 °C for 1 h. The HA titer was identified as the reciprocal of the highest antigen dilution showing complete agglutination of the erythrocytes [31, 32].

## Results

### Dissecting the effects of DVG 2.2 on the synthesis of IFN $\beta$ and ISG15 mRNAs

The synthesis of different defective viral genomes (DVGs) with various RNA structures is a feature of RNA virus infection, including coronavirus infection [33, 34]. A previous study suggested that the synthesized coronavirus DVGs in infected cells can collectively induce interferon signaling based on a transcriptome analysis [26]; however, because (i) RNA structures are associated with the activation of interferon signaling [17–20] and (ii)

coronavirus DVGs can encode proteins [35], it remains to be clarified whether the induction of interferon signaling is derived from the DVG at the level of RNA or protein or both. In addition, because (i) HEK-293T cells have a high transfection efficiency [36], (ii) bovine coronavirus (BCoV) can replicate in HEK-293T cells, and (iii) IFN $\beta$  and downstream ISG15 mRNAs can also be synthesized in HEK-293T cells in response to stimulation [37, 38], HEK-293T cells and BCoV were selected for this study. Therefore, DVG 2.2, which was previously identified in BCoV-infected cells [8, 29], was selected and examined in HEK-293T cells. DVG 2.2, which consists

of genes encoding partial nsp1 and complete nucleocapsid protein, and both 5' and 3' UTRs at the terminus (Fig. 1A), has been employed as a surrogate of the

coronavirus full-length genome for the study of coronavirus gene expression [29, 35, 39–44]. This DVG can encode an in-frame fusion protein containing partial nsp1 and a complete nucleocapsid protein with a molecular weight of ~60.5 kDa (Fig. 1A). Consequently, to clarify that the induction of interferon signaling (Fig. 1B) by DVG 2.2 is at the level of the RNA, protein or both, DVG 2.2 with a stop codon downstream of the start codon was constructed (designated  $\Delta$ DVG 2.2) (Fig. 1A). The in vitro-transcribed DVG 2.2 and  $\Delta$ DVG 2.2 were then respectively transfected into HEK-293T cells, and cellular protein and RNA were collected at 24 h post transfection (hpt) to detect protein synthesis via Western blot and the synthesis of IFN $\beta$  and ISG15 mRNAs via RT-qPCR (Fig. 1B and C). As shown in Fig. 1D, DVG-expressed

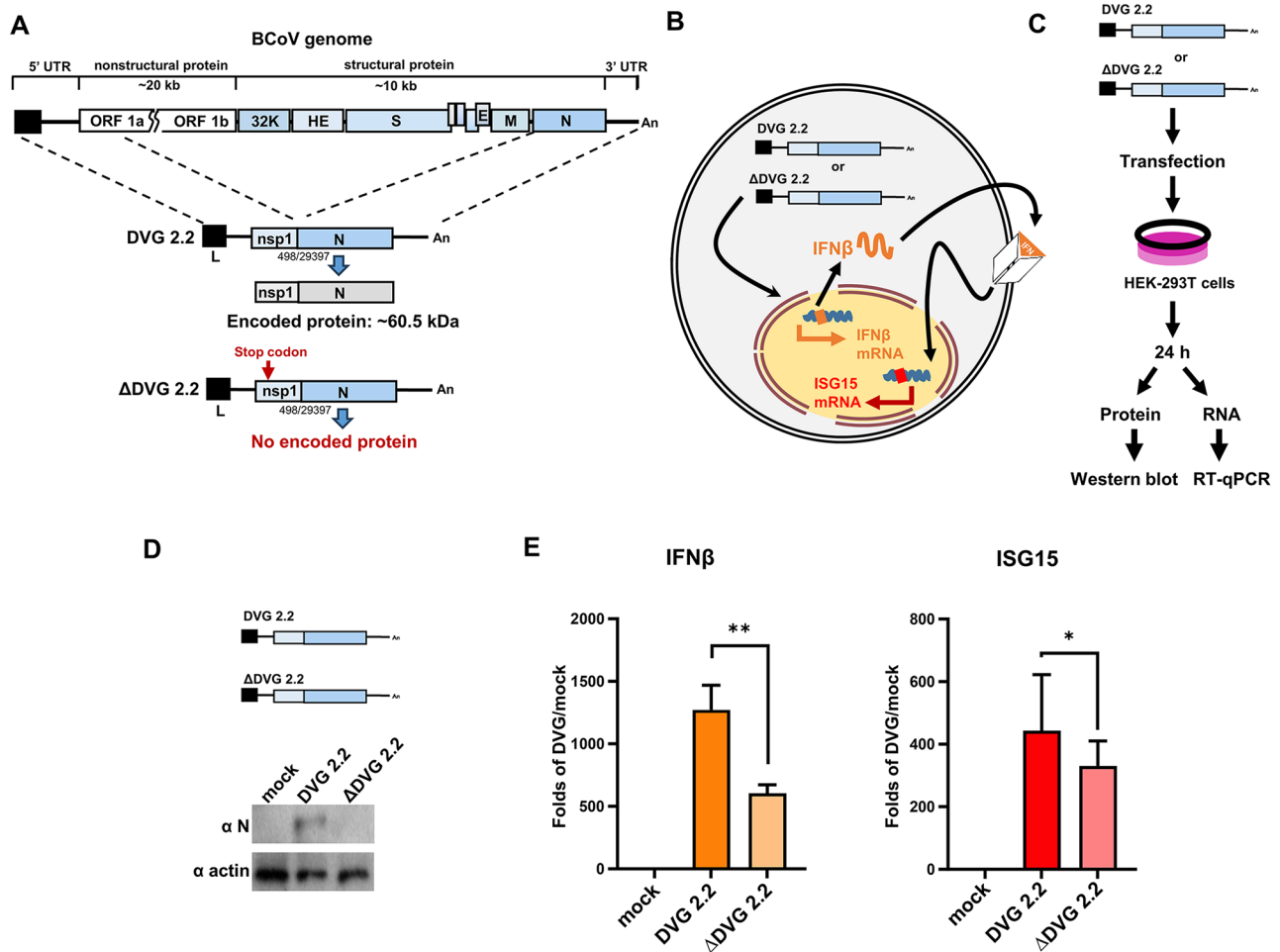


**Fig. 1** Dissecting the effects of DVG 2.2 on the synthesis of IFN $\beta$  and ISG15 mRNAs. **(A)** The genome structure of BCoV, DVG 2.2 and  $\Delta$ DVG 2.2. DVG 2.2 consists of partial nsp1 and the complete nucleocapsid protein-encoding gene, and the UTR at its 5' and 3' termini is expected to encode a fusion protein of ~60.5 kDa. The numbers shown in each DVG structure are the nucleotide positions at which recombination occurred. The  $\Delta$ DVG 2.2 has a stop codon downstream of the start codon and thus is expected to lose its protein-coding ability. **(B)** Schematic diagram depicting IFN $\beta$  signaling and its downstream interferon-stimulated gene ISG15 induced by DVG 2.2 or  $\Delta$ DVG 2.2. **(C)** Diagram depicting the experimental procedure used to examine the effects of DVG 2.2 or  $\Delta$ DVG 2.2 on interferon signaling. **(D)** Detection of proteins encoded by DVG 2.2 and  $\Delta$ DVG 2.2 by Western blot. **(E)** Comparison of the relative expression of IFN $\beta$  mRNA (left panel) and ISG15 mRNA (right panel) between DVG 2.2- and  $\Delta$ DVG 2.2-transfected HEK-293T cells. "Mock" indicates the amount of mRNA detected from mock-transfected cells. The "Folds of DVG/mock" on the y-axis is presented as relative units of mRNA compared with the amount of mRNA in mock-transfected cells (the amount of mRNA in mock-transfected cells = 1). \* $p < 0.05$ , \*\* $p < 0.01$

proteins were detected in DVG 2.2-, but not  $\Delta$ DVG 2.2-, transfected HEK-293T cells. Compared with that in mock-transfected cells, an increase (~605-fold) in IFN $\beta$  mRNA in cells transfected with  $\Delta$ DVG 2.2 was observed after 24 h of transfection (Fig. 1E, left panel). Similar increases also occurred in ISG15 mRNA levels (~330-fold) (Fig. 1E, right panel). In addition, compared with those in mock-transfected cells, the levels of IFN $\beta$  (~1272-fold) and ISG15 (~443-fold) mRNAs in cells transfected with DVG 2.2 were also greater than those in mock-transfected cells. These results together suggested that DVG 2.2 at the level of RNA ( $\Delta$ DVG 2.2, Fig. 1E) and DVG 2.2 at the level of both the RNA and protein combined (DVG 2.2, Fig. 1E) can induce the interferon signaling pathway. Furthermore, the synthesis of IFN $\beta$  mRNA in DVG 2.2-transfected cells (~1272-fold) was greater than that (~605-fold) in  $\Delta$ DVG 2.2-transfected cells, as was the synthesis of ISG15 mRNA (~330-fold in  $\Delta$ DVG 2.2-transfected cells vs. ~443-fold in DVG 2.2-transfected cells). Consequently, because the synthesis of IFN $\beta$  and ISG15 mRNAs was greater in DVG 2.2-transfected cells (at the level of both the RNA and the protein combined) than in  $\Delta$ DVG 2.2-transfected cells (at the level of only RNA), the results may also suggest that the DVG 2.2-expressing protein potentially has positive effect on the induction of interferon signaling. Together, these results suggest that DVG 2.2 can induce interferon signaling at the RNA, protein and combined levels.

#### The effects of DVG 2.2 on coronavirus replication vary under different infection conditions

Since DVG 2.2 can induce interferon signaling, we next examined whether DVG 2.2-induced interferon signaling can inhibit coronavirus RNA synthesis. To this end, DVG 2.2 was first transfected into HEK-293T cells, and at 24 hpt, the cells were infected with BCoV. At 8 h postinfection (hpi), supernatant and total cellular RNA were collected (Fig. 2A). RT-qPCR revealed that the RNA synthesis of BCoV was inhibited (Fig. 2B, upper panel), as were the viral titers (Fig. S7A), in the presence of DVG 2.2 at 8 hpi. Moreover, during RNA collection, the IFN $\beta$  and ISG15 mRNAs in DVG 2.2-transfected and BCoV-infected cells (Fig. 2B, middle and lower panels, respectively) were also increased compared with those in mock-transfected BCoV-infected HEK-293T cells. These results suggested that DVG 2.2 can inhibit coronavirus RNA synthesis and that this inhibitory effect is correlated with the level of interferon signaling based on the increased amounts of the IFN $\beta$  and ISG15 mRNAs (Fig. 2B, middle and lower panels, respectively). Furthermore, because DVGs can be synthesized during coronavirus infection, it remains to be determined whether DVGs still have an inhibitory effect on coronavirus replication when cells have been previously infected with

coronavirus. To examine this possibility, HEK-293T cells were first infected with BCoV, and at 3, 5 and 8 hpi, the cells were then transfected with DVG 2.2, followed by RT-qPCR to evaluate the efficiency of BCoV RNA synthesis (Fig. 2C). The results, as shown in Fig. 2D, suggested that, in comparison with that in mock-transfected cells, the BCoV RNA synthesis was slightly increased in DVG 2.2-transfected cells that had been first infected with BCoV for 3 h (Fig. 2D, upper panel). However, the BCoV RNA synthesis was inhibited in DVG 2.2-transfected cells that had been first infected with BCoV for 5 and 8 h (Fig. 2D, upper panel). The virus titers were decreased in DVG 2.2-transfected cells that had been first infected with BCoV for 3, 5 and 8 h (Fig. S7B). In addition, although both the IFN $\beta$  and ISG15 mRNAs in DVG 2.2-transfected cells were still detected, the inhibitory effect on BCoV RNA synthesis was not correlated with the level of interferon signaling (Fig. 2D, middle and lower panels). It is speculated that the effects of DVG 2.2 at the RNA, protein or combined level on cells may be altered when cells are first infected with coronavirus followed by transfection, leading to different effects of DVG 2.2 on BCoV RNA synthesis and titers under different infection conditions (for a detailed explanation, please see the discussion). Together, these results suggest that although DVG 2.2 has the ability to inhibit coronavirus RNA synthesis and titers, its effect on coronavirus replication varies under different infection conditions.

#### Dissecting the effects of DVG 5.1 on the synthesis of IFN $\beta$ and ISG15 mRNAs

DVG 5.1 (Fig. 3A), which is also a BCoV-derived DVG and was identified from a previous study [8], consists of genes encoding complete nsp1; parts of the nsp2, nsp14, nsp15 and E proteins; the complete M and N proteins; and UTRs at its 5' and 3' termini (Fig. 3A). During the synthesis of DVG 5.1, a stop codon was introduced into the nsp14 gene due to recombination, resulting in the fusion protein encoded from DVG 5.1 containing complete nsp1, partial nsp2 and out-of-frame nsp14 with a molecular weight of ~36.7 kDa (Fig. 3A). To examine whether DVG 5.1, which has a different genome structure than DVG 2.2, has a similar behavior to that of DVG 2.2 in terms of its effect on the synthesis of IFN $\beta$  and ISG15 mRNAs (Fig. 3B) at the level of RNA or protein or both, a stop codon was also introduced into DVG 5.1 (designated  $\Delta$ DVG 5.1, Fig. 3A) to block protein synthesis, followed by the transfection of DVG 5.1 or  $\Delta$ DVG 5.1.

(Fig. 3C). As shown in Fig. 3D, DVG-expressing proteins were detected in DVG 5.1-transfected but not in  $\Delta$ DVG 5.1-transfected HEK-293T cells. RT-qPCR (Fig. 3E, left panel) revealed an increase (~34-fold) in IFN $\beta$  mRNA in cells transfected with DVG 5.1 compared with mock-transfected cells. Interestingly, the

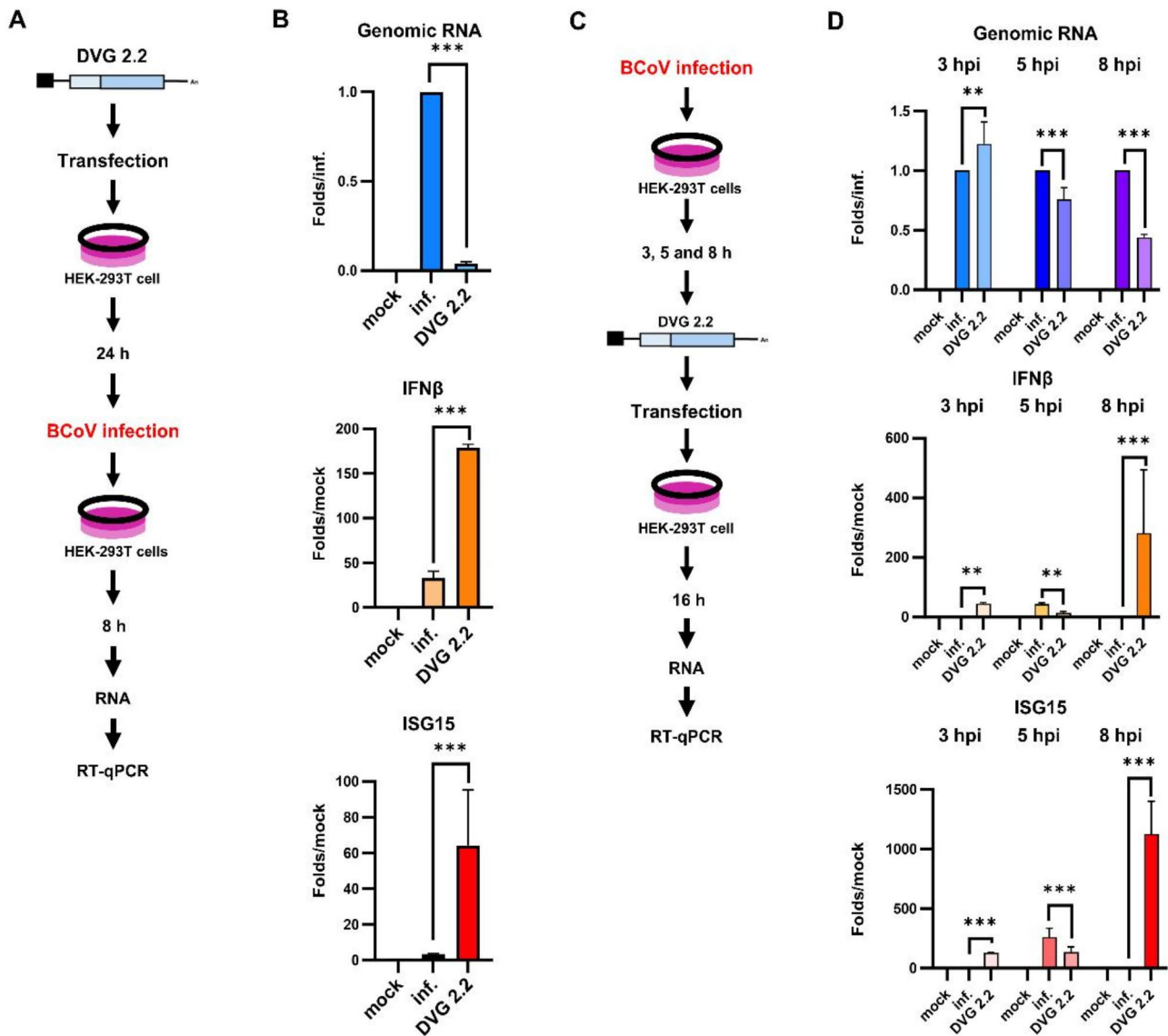


**Fig. 2** The effect of DVG 2.2 on coronavirus RNA synthesis under different infection conditions. **(A)** and **(C)** Diagram depicting the experimental procedure used to examine the effects of DVG 2.2 on coronavirus RNA synthesis, in which DVG 2.2 transfection was performed before **(A)** or after **(C)** BCoV infection. **(B)** and **(D)** Comparison of the relative amounts of BCoV RNA, IFN- $\beta$  mRNA and ISG15 mRNA between mock-transfected (inf) and DVG 2.2-transfected (DVG 2.2) HEK-293T cells infected with BCoV after **(B)** or before **(D)** transfection. "Mock" indicates that the HEK-293T cells were mock-transfected and mock-infected. Upper panel: The "Folds/inf." on the y-axis is presented as relative units of BCoV RNA in DVG 2.2-transfected and BCoV-infected cells compared with the amount of BCoV RNA in mock-transfected and BCoV-infected cells (the amount of BCoV RNA in mock-transfected and BCoV-infected cells (inf) = 1). Middle and lower panels: The "Folds/mock" on the y-axis is presented as relative units of mRNA compared with the amount of mRNA in mock-transfected and mock-infected cells (the amount of mRNA in mock-transfected and mock-infected cells (mock) = 1). \*\* $p < 0.01$ , \*\*\* $p < 0.001$

synthesis of IFN $\beta$  mRNA in DVG 5.1-transfected cells (~34-fold) was lower than that in  $\Delta$ DVG 5.1-transfected cells (~230-fold). Similar results were also observed for the synthesis of ISG15 mRNA (~90-fold in DVG 5.1-transfected cells vs. ~330-fold in  $\Delta$ DVG 5.1-transfected cells) (Fig. 3E, right panel). These results, similar to those derived from DVG 2.2, suggested that, either at the level of RNA or at the level of both the RNA and protein combined, DVG 5.1 can induce interferon signaling. However, in contrast to the results derived from DVG

2.2, the activation strength at the combined level of both RNA and protein (DVG 5.1) was lower than that at the level of only RNA ( $\Delta$ DVG 5.1). Based on these results, we suggested that the DVG 5.1-expressed protein may have a negative effect on the induction of interferon signaling. Consequently, dissecting the function of DVG 5.1 in interferon signaling suggested that DVG 5.1 can induce interferon signaling at the level of RNA and at the level of both the RNA and protein combined; however, DVG5.1 at the level of its encoded protein may have a negative

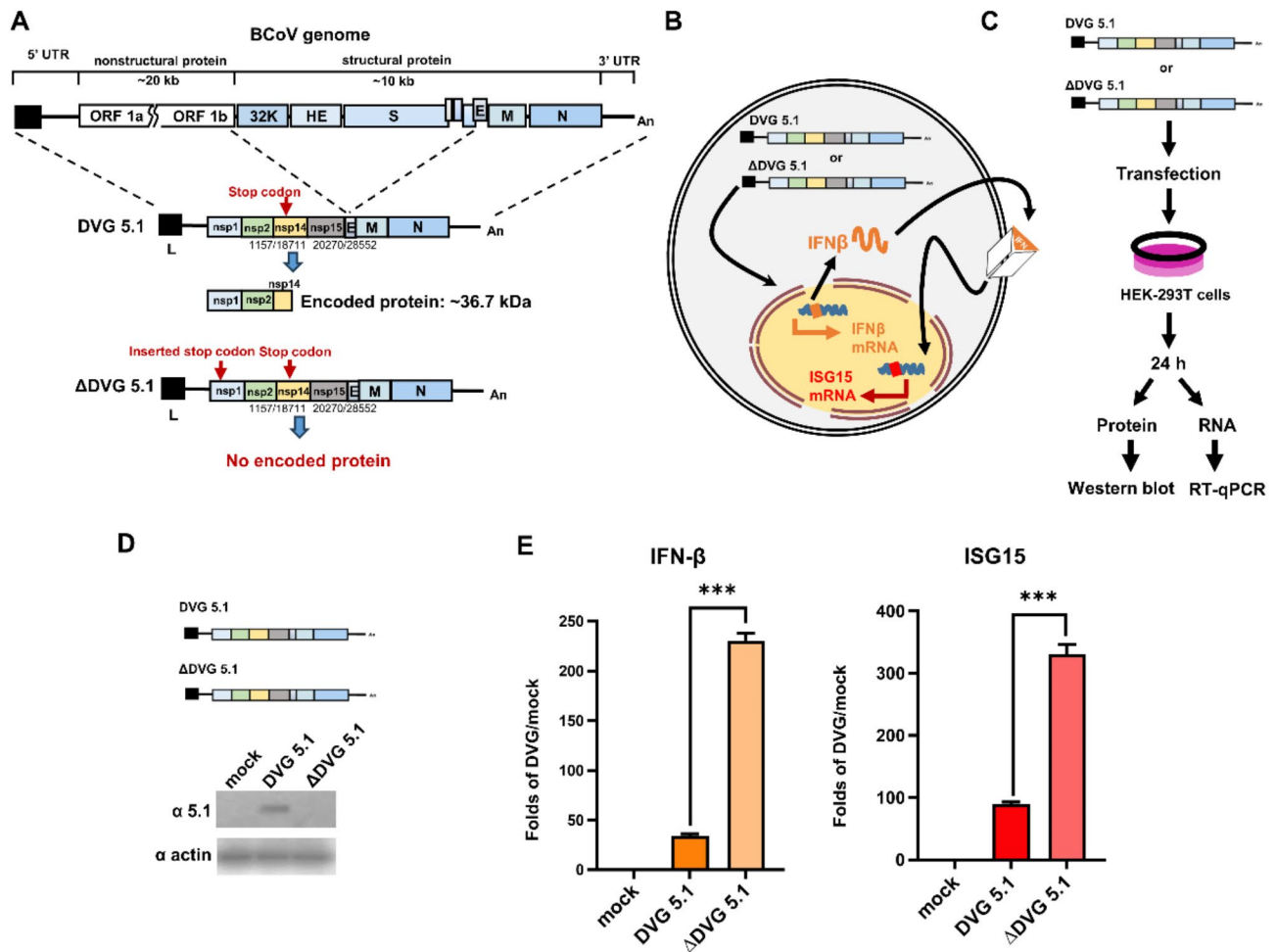


**Fig. 3** Dissecting the effects of DVG 5.1 on the synthesis of IFN $\beta$  and ISG15 mRNAs. **(A)** The genome structure of BCoV, DVG 5.1 and  $\Delta$ DVG 5.1. DVG 5.1, which consists of genes encoding complete nsp1; parts of nsp2, nsp14, nsp15 and the E protein; complete M and N proteins; and UTRs at the 5' and 3' termini, is expected to encode fusion proteins of ~36.7 kDa. The numbers shown in each DVG structure are the nucleotide positions at which recombination occurred. The  $\Delta$ DVG 5.1 has a stop codon downstream of the start codon and thus is expected to lose protein-coding ability. **(B)** Schematic diagram depicting IFN $\beta$  signaling and its downstream interferon-stimulated gene ISG15 induced by DVG 5.1 or  $\Delta$ DVG 5.1. **(C)** Diagram depicting the experimental procedure used to examine the effects of DVG 5.1 or  $\Delta$ DVG 5.1 on interferon signaling. **(D)** Detection of proteins encoded by DVG 5.1 and  $\Delta$ DVG 5.1 by Western blot. **(E)** Comparison of the relative expression of IFN $\beta$  mRNA (left panel) and ISG15 mRNA (right panel) between DVG 5.1- and  $\Delta$ DVG 5.1-transfected HEK-293T cells. "Mock" indicates the amount of mRNA detected from mock-transfected cells. The "Folds of DVG/mock" on the y-axis is presented as relative units of mRNA compared with the amount of mRNA in mock-transfected cells (the amount of mRNA in mock-transfected cells = 1). \*\*\* $p < 0.001$

effect on interferon signaling based on the amounts of the IFN $\beta$  and ISG15 mRNAs (Fig. 3E).

**The effects of DVG 5.1 on coronavirus replication efficiency also vary under different infection conditions**

The results of the previous study shown in Fig. 2 suggest that DVG 2.2 can inhibit coronavirus replication, although its effects on coronavirus replication vary under different infection conditions. Consequently, to further examine whether DVG 5.1 has similar effects on the inhibition of coronavirus replication under different infection conditions, DVG 5.1 was first transfected into HEK-293T cells for 24 h, followed by infection with BCoV, and supernatant and RNA were collected at 8 hpi followed by RT-qPCR and HA assay (Fig. 4A and Fig. S8A). As shown

in Fig. 4B and Fig. S8A, the efficiency of BCoV RNA synthesis and the virus titers, respectively, was lower in DVG 5.1-transfected and BCoV-infected cells than in mock-transfected and BCoV-infected cells. In addition, compared with those in mock-transfected and BCoV-infected cells, increases in both the IFN $\beta$  and ISG15 mRNAs were detected in DVG 5.1-transfected and BCoV-infected cells. These results suggested that, similar to DVG 2.2, DVG 5.1 has the ability to inhibit coronavirus RNA synthesis and that this inhibitory effect is also correlated with the level of interferon signaling based on the increased amounts of the IFN $\beta$  and ISG15 mRNAs (Fig. 4B, middle and lower panels, respectively). On the other hand, the previous results for DVG 2.2 also suggested that the efficiency of coronavirus RNA synthesis and virus titers in cells firstly

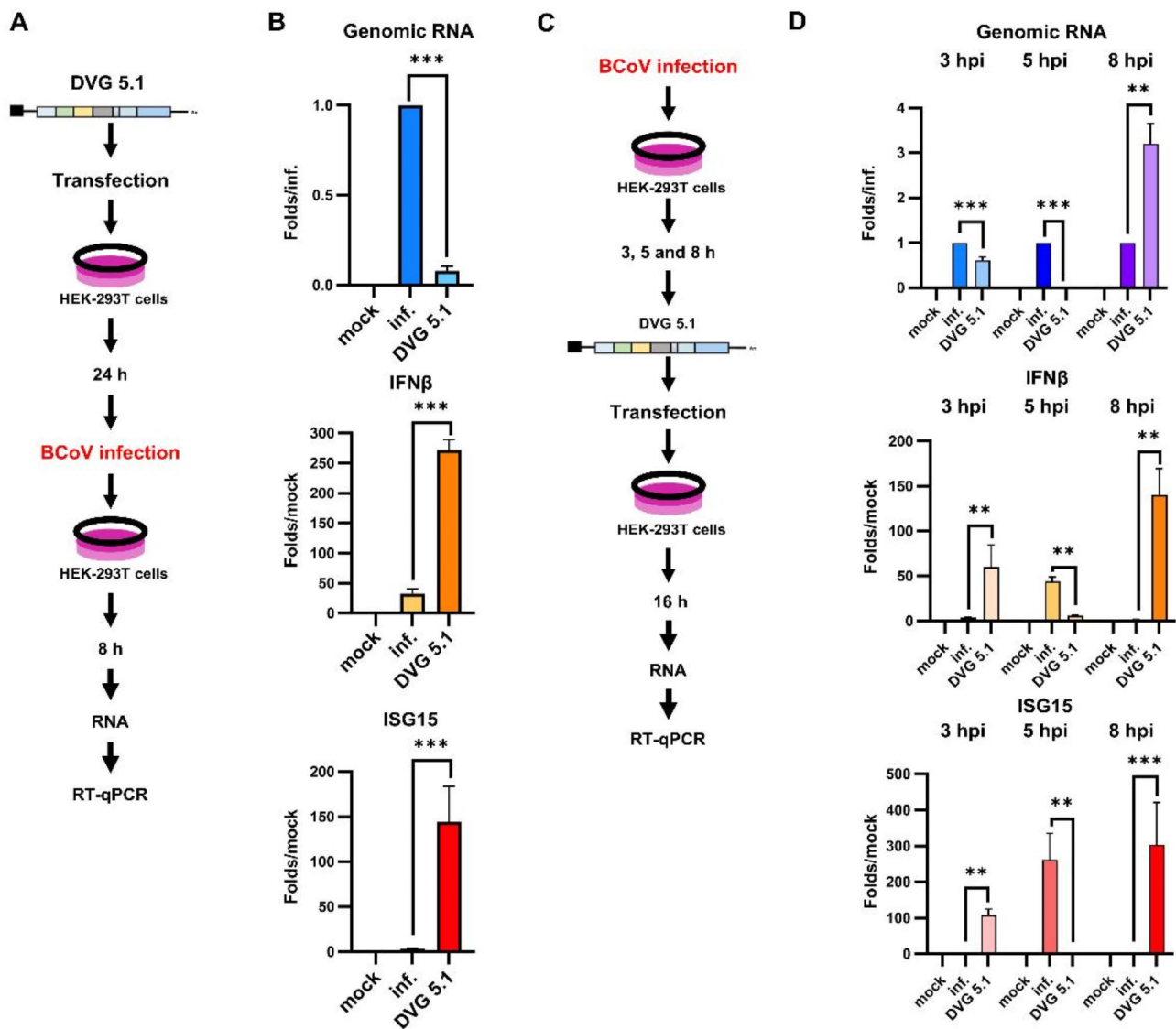


**Fig. 4** The effect of DVG 5.1 on coronavirus RNA synthesis under different infection conditions. (A) and (C) Diagram depicting the experimental procedure used to examine the effects of DVG 5.1 on BCoV RNA synthesis, in which DVG 5.1 transfection was performed before (A) or after (C) BCoV infection. (B) and (D) Comparison of the relative amounts of BCoV RNA, IFN- $\beta$  mRNA and ISG15 mRNA between mock-transfected (inf.) and DVG 5.1-transfected (DVG 5.1) HEK-293T cells infected with BCoV after (B) or before (D) transfection. "Mock" indicates that the HEK-293T cells were mock-transfected and mock-infected. Upper panel: The "Folds/inf." on the y-axis is presented as relative units of BCoV RNA in DVG 5.1-transfected and BCoV-infected cells compared with the amount of BCoV RNA in mock-transfected and BCoV-infected cells (the amount of BCoV RNA in mock-transfected and BCoV-infected cells (inf.) = 1). Middle and lower panels: The "Folds/mock" on the y-axis is presented as relative units of mRNA compared with the amount of mRNA in mock-transfected and mock-infected cells (the amount of mRNA in mock-transfected and mock-infected cells (mock) = 1). \*\* $p < 0.01$ , \*\*\* $p < 0.001$

infected with BCoV followed by the transfection varied in comparison with that in cells firstly infected with BCoV followed by the mock transfection (Fig. 2D, upper panel). To examine whether similar results can occur for DVG 5.1, HEK-293T cells were first infected with BCoV followed by the transfection or mock-transfection of DVG 5.1 (Fig. 4C). Compared with that in mock-transfected and BCoV-infected cells, the efficiency of BCoV RNA synthesis (Fig. 4D, upper panel) and virus titers (Fig. S8B) was inhibited in DVG 5.1-transfected and BCoV-infected

cells, which were first infected with BCoV for 3 and 5 h. However, the efficiency of BCoV RNA synthesis slightly increased in transfected cells that were first infected with BCoV for 8 h (Fig. 4D, upper panel) although virus titers were still decreased (Fig. S8B). In addition, the inhibitory effect on BCoV RNA synthesis was not correlated with the levels of both the IFN $\beta$  and ISG15 mRNAs (Fig. 4D, middle and lower panels). Consequently, similar to the results acquired from DVG 2.2, those derived from DVG 5.1 suggest that DVG 5.1 also has the ability to inhibit

coronavirus RNA synthesis and titers and that the inhibition efficiency varies when cells are infected with BCoV before or after transfection.

#### **Effects of different DVG species on the synthesis of IFN $\beta$ and ISG15 mRNAs and coronavirus replication**

Previous studies have revealed that many DVG species with a variety of genome structures can be produced in coronavirus-infected cells [8, 9]. To further explore whether different DVG species have different effects on the synthesis of IFN $\beta$  and ISG15 mRNAs, a series of DVGs (Fig. 5A) were selected and constructed on the basis of the results of identified DVG species in a previous study [8]. The selected DVGs have the following features in common: (i) they all have 5' and 3' UTRs, and (ii) they all have the potential to encode fusion proteins. The differences are as follows: (i) the selected DVGs all contain both nsp and N protein genes, but the lengths of nsp and N protein genes are different, and (ii) the selected DVGs contain in-frame (DVG 678, DVG 722, DVG 823, DVG 930, DVG 1066, DVG 378, DVG 825, DVG 836 and DVG 2.2) or out-of-frame (DVG 857 and DVG 5.1) ORFs compared with the full-length BCoV genome structure. Consequently, to examine whether the different DVGs with different genome structures had different effects on the synthesis of IFN $\beta$  and ISG15 mRNAs, these DVGs were respectively transfected into HEK-293 cells, followed by RNA collection at 24 hpt and RT-qPCR (Fig. 5B). As shown in Fig. 5C, the selected DVGs all induced the synthesis of IFN $\beta$  and ISG15 mRNAs, at 24 hpt, although the induced strength varied among the selected DVGs. Notably, the amount of the expressed IFN $\beta$  mRNA was correlated with that of the expressed ISG15 mRNA overall for each of the selected DVGs, even though the expressed amounts varied among the selected DVGs. On the basis of the results above, all the selected DVGs can induce interferon signaling on the basis of the amounts of IFN $\beta$  and ISG15 mRNAs, although the induced strength varies among the selected DVGs.

To further examine whether the selected DVGs have the ability to affect coronavirus RNA synthesis and virus titers, the selected DVGs (Fig. 5A) were also respectively transfected into HEK-293T cells, and at 24 hpt, the cells were infected with BCoV, followed by supernatant and RNA collection at 4 and 8 hpi (Fig. 5D and Fig. S9B). As shown in Fig. 5E, the synthesis efficiency of BCoV RNA decreased at different levels among the selected DVGs. However, the decreased levels of coronavirus RNA synthesis (Fig. 5E) and titer (Fig. S9C) among the selected DVGs were not always closely related (for a detailed explanation, please see the discussion). Together, the results shown in Fig. 5C and E suggested that the selected DVGs all have the ability to affect coronavirus replication, including RNA synthesis and titers, at least partly

through the induction of interferon signaling, although the strength of the induction of interferon signaling and efficiency of coronavirus RNA synthesis is not closely related. Combined, similar to DVG 5.1 and DVG 2.2, the selected DVGs can induce interferon signaling in terms of the synthesis of IFN $\beta$  and ISG15 mRNAs, and have the ability to affect coronavirus replication when cells are first transfected with DVG followed by infection with BCoV, although the aforementioned effects among the selected DVGs are diverse.

#### **Different DVG species have different inhibitory effects on coronavirus replication under different infection conditions**

The results of the previous experiments (Figs. 2B, 4B and 5E) suggest that coronavirus DVG can inhibit coronavirus replication when DVG is first transfected into cells, followed by infection with coronavirus. Because DVG can be synthesized during infection, we also examined whether DVGs 5.1 and 2.2 still have an inhibitory effect on coronavirus RNA synthesis and titers when cells have been previously infected with coronavirus for different periods of time; however, the results suggested that the inhibitory effect varies between DVG 5.1 and 2.2 under such infection conditions (Figs. 2D and 4D). It is therefore speculated that the inhibitory effect may also vary between the different DVG species when cells are first infected with coronavirus followed by the transfection of respective DVGs. To this end, HEK-293T cells were first infected with BCoV, and at 3, 5 and 8 hpi, the cells were then transfected with the respective DVGs for 16 h, followed by RT-qPCR and HA assay to evaluate their ability to inhibit BCoV replication (Fig. 6B and S10B). As shown in Fig. 6C and E, left panel and Fig. S10C, compared with mock-transfected BCoV-infected cells, the selected DVG species presented different levels of BCoV replication including RNA synthesis and virus titers when the cells had been previously infected with BCoV for different periods of time. Overall, some of the selected DVGs (DVG 678, DVG 823 and DVG 930) had no inhibitory effect on BCoV RNA synthesis, but the others had such inhibitory effects, although the inhibition occurred at different time points of postinfection (3, 5 and 8 hpi) prior to transfection (Fig. 6E, left panel). In addition, the levels of IFN $\beta$  and ISG15 mRNA synthesis also varied and were not always correlated with the levels of BCoV RNA synthesis efficiency (Fig. 6D, E and F, middle and right panels). In terms of the individual selected DVGs, the inhibitory patterns varied at different time points of postinfection (3, 5 and 8 hpi) prior to transfection (DVG 722, DVG 1066, DVG 378, DVG 825, DVG 836, DVG 857, DVG 2.2 and DVG 5.1) (Fig. 6E, left panel). Specifically, the efficiency of BCoV RNA synthesis increased and then gradually decreased (DVG 722, DVG 1066 and DVG

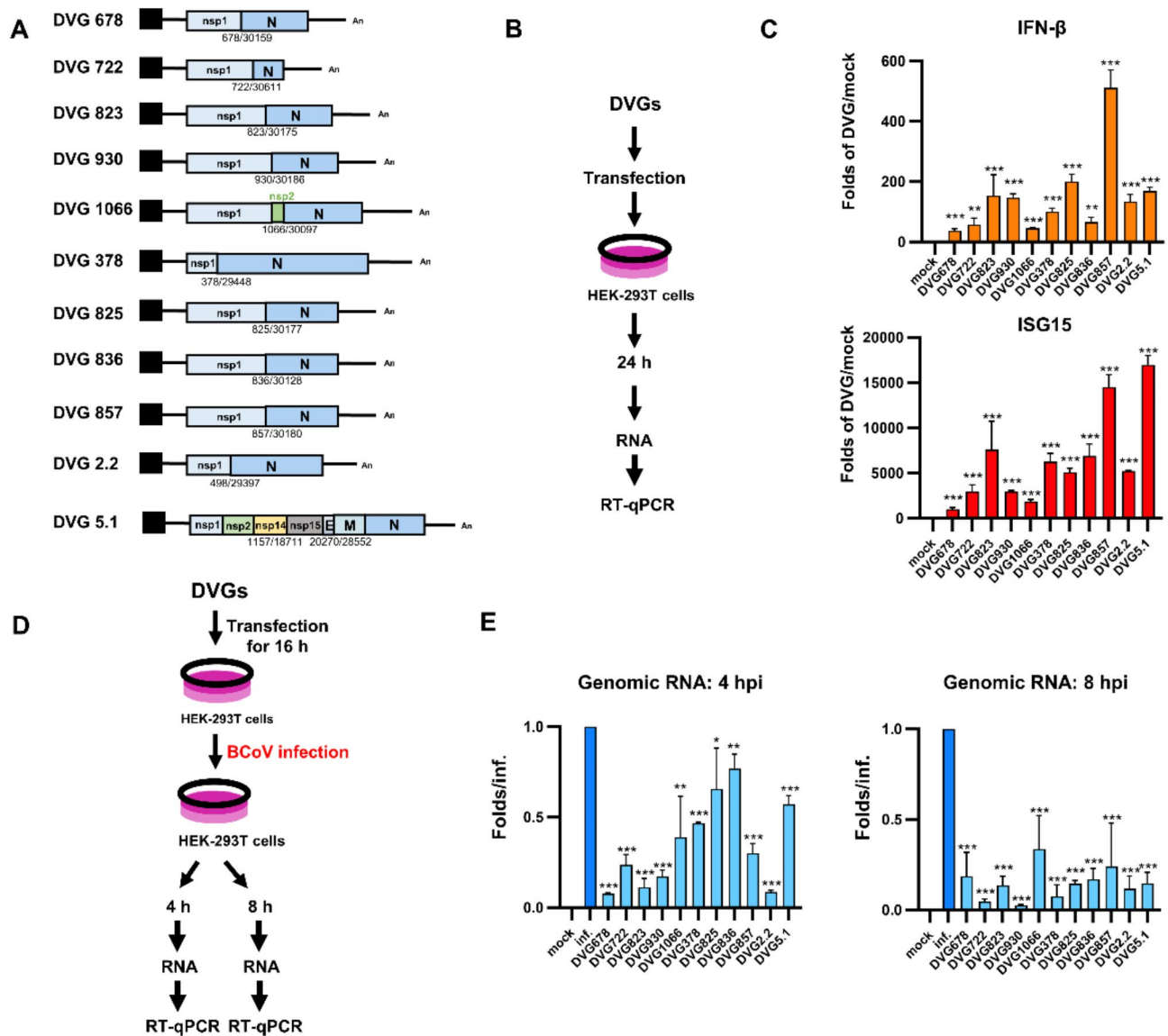


**Fig. 5** Effects of different DVG species on interferon signaling and coronavirus RNA synthesis. **(A)** The genome structures of the naturally occurring BCoV DVGs selected for this experiment. The numbers shown in each DVG structure are the nucleotide positions at which recombination occurred. **(B)** Diagram depicting the experimental procedure used to examine the effects of the selected DVG species on interferon signaling. **(C)** Comparison of the relative expression of IFN $\beta$  mRNA (upper panel) and ISG15 mRNA (lower panel) between mock-transfected HEK-293T cells and HEK-293T cells respectively transfected with the selected DVGs shown in (A). “Mock” indicates the amount of mRNA detected from mock-transfected cells. The “Folds of DVG/mock” on the y-axis is presented as relative units of mRNA compared with the amount of mRNA in mock-transfected cells (the amount of mRNA in mock-transfected cells = 1). **(D)** Diagram depicting the experimental procedure used to examine the effects of selected DVGs on BCoV RNA synthesis, in which the transfection of selected DVGs was performed before BCoV infection. **(E)** Comparison of the relative amounts of BCoV RNA between mock-transfected (inf.) and DVG-transfected HEK-293T cells infected with BCoV after transfection. “Mock” indicates that the HEK-293T cells were mock-transfected and mock-infected. The “Folds/inf.” on the y-axis is presented as relative units of BCoV RNA compared with the amount of BCoV RNA in mock-transfected and BCoV-infected cells (the amount of BCoV RNA in mock-transfected and BCoV-infected cells (inf.) = 1). \* $p < 0.05$ , \*\* $p < 0.01$ , \*\*\* $p < 0.001$

857); the efficiency of BCoV RNA synthesis increased, decreased and then increased at different time points of postinfection prior to infection (DVG 378); and the efficiency of BCoV RNA synthesis decreased and then gradually increased (DVG 825). Note that the inhibitory effects of DVG 2.2 and DVG 5.1 on BCoV RNA synthesis have been described in Figs. 2D and 4D. On the other

hand, different DVG species also had different effects on the virus titers (Fig. S10C) although the decreased levels of the coronavirus RNA synthesis (6 C and 6E, left panel) and titer (Fig. S10C) among the selected DVGs were not always closely related. Consequently, these results together suggest that (i) different DVG species have different effects on the efficiency of BCoV replication,

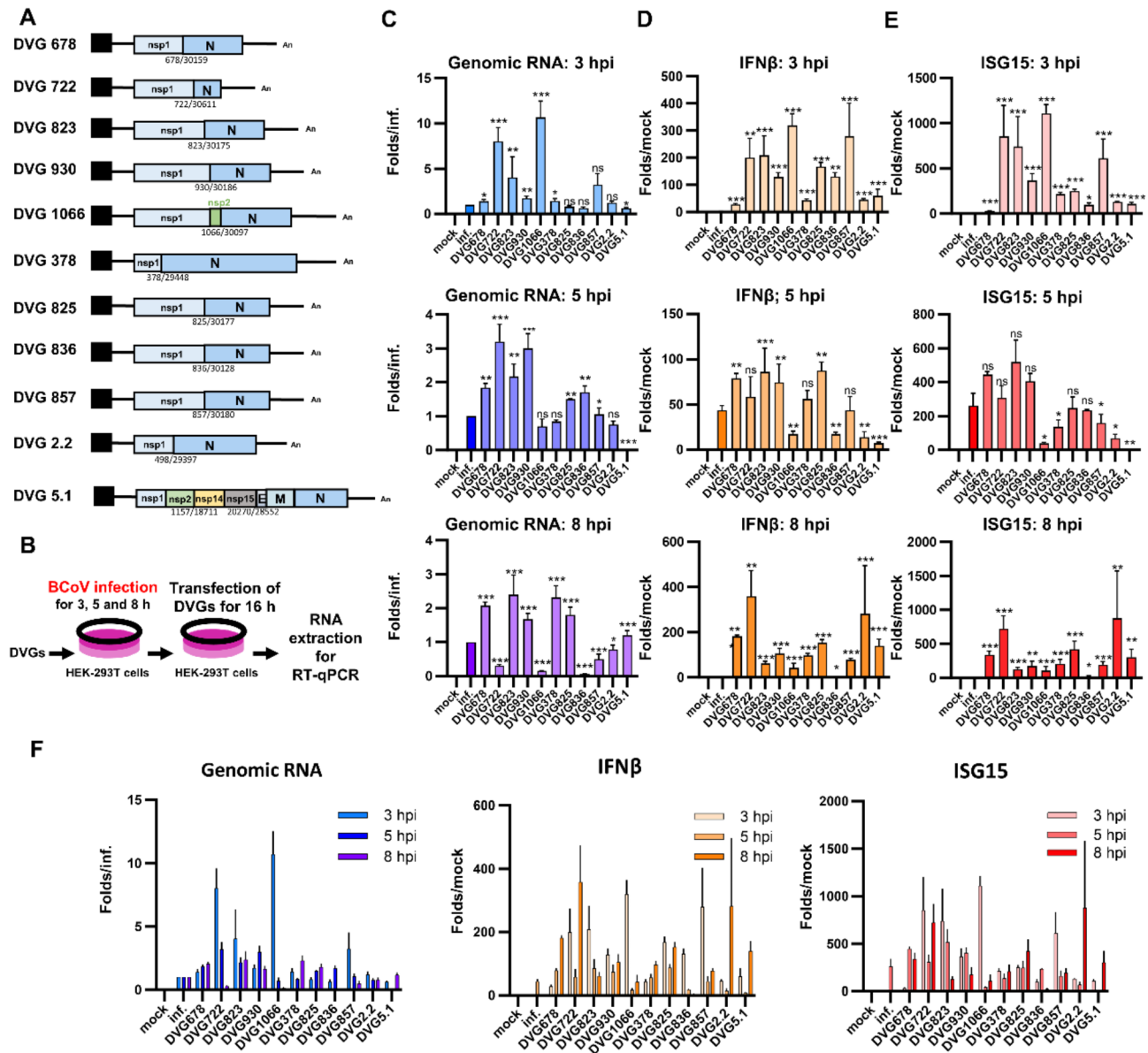


**Fig. 6** Effect of different DVG species on coronavirus RNA synthesis in HEK-293T cells in which transfection is performed after infection. **(A)** The genome structures of the naturally occurring BCoV DVGs selected in the experiment. The numbers shown in each DVG structure are the nucleotide positions at which recombination occurred. **(B)** Diagram depicting the experimental procedure used to examine the effects of the selected DVGs on BCoV RNA synthesis, in which DVG transfection is performed after BCoV infection. **(C)** Comparison of the relative amounts of BCoV RNA between mock-transfected and DVG-transfected HEK-293T cells that were first infected with BCoV and then respectively transfected with the selected DVGs at 3 (upper panel), 5 (middle panel) and 8 (lower panel) hpi. “Mock” indicates that the HEK-293T cells were mock-transfected and mock-infected. The “Folds/inf.” on the y-axis is presented as relative units of BCoV RNA compared with the amount of BCoV RNA in mock-transfected and BCoV-infected cells (the amount of BCoV RNA in mock-transfected and BCoV-infected cells (inf.) = 1). **(D)** and **(E)** Comparison of the relative expression of IFNβ mRNA **(D)** and ISG15 mRNA **(E)** between mock-transfected HEK-293T cells and DVG-transfected HEK-293T cells, which were first infected with BCoV and then respectively transfected with the selected DVGs at 3, 5 and 8 hpi. The “Folds/mock” on the y-axis is presented as relative units of mRNA compared with the amount of mRNA in mock-transfected and mock-infected cells (the amount of mRNA in mock-transfected and mock-infected cells (mock) = 1). **(F)** Summary of the data derived from **(C)**-**(E)** showing the different effects of the individual DVG species on BCoV RNA synthesis (left panel) and on interferon signaling (middle and right panels) in HEK-293T cells, which were first infected with BCoV and then transfected with DVG at 3, 5 and 8 hpi. ns, not significant. \* $p < 0.05$ , \*\* $p < 0.01$ , \*\*\* $p < 0.001$

including RNA synthesis and virus titers and (ii) the levels of IFN $\beta$  and ISG15 mRNA synthesis are not always correlated with the levels of the efficiency of BCoV replication in the environment where cells are first infected with coronavirus, followed by the transfection of DVGs.

### Coronavirus DVGs can collectively affect coronavirus replication

It has been documented that DVGs are synthesized abundantly, but the number of individual DVGs is not high in coronavirus-infected cells [8]. Consequently, it is speculated that DVGs may exert their functions on coronavirus and host cells collectively but not individually. Thus, to examine whether coronavirus DVGs still has an inhibitory effect on coronavirus replication when different DVG species are transfected together into the same cultured cells, the selected DVGs shown in Fig. 7A were mixed together (100 ng for each DVG) and then transfected into HEK-293T cells that had been infected with BCoV for 3, 5 or 8 h. After 16 h of transfection, RNA and supernatant were collected and subjected to RT-qPCR and HA assay (Fig. 7B and S11B). As shown in Fig. 7C, an inhibitory effect was observed at 3 and 5, but not 8 hpi prior to transfection, and the levels of IFN $\beta$  and ISG15 mRNA synthesis (Fig. 7D and E) were not correlated with the inhibition levels of BCoV RNA synthesis (Fig. 7C). In addition, the virus titers were all decreased at 3, 5 and 8 hpi prior to transfection (Fig. S11C). Thus, the selected coronavirus DVG still has an inhibitory effect on coronavirus replication when a population of DVG species are present in the same cultured cells. The inhibitory results were also obtained when DVGs with no 5' or 3' UTRs or both UTRs (Fig. 7F and S11D) were transfected together into the same cultured cells which have been infected by BCoV for 8 h (8 hpi) (Fig. 7H, left panel and S11F). In addition, the levels of IFN $\beta$  and ISG15 mRNA synthesis (Fig. 7H, middle and right panels) were not correlated with the inhibition levels of BCoV RNA synthesis and titer (Fig. 7H, left panel and S11F). Note that DVG 30,015, DVG 1353 and DVG 472 contain in-frame ORFs and DVG 30,073, DVG 1557 and DVG 314 contain out-of-frame ORFs. Consequently, DVGs can collectively affect coronavirus RNA replication, although their inhibitory strength is not correlated with the levels of IFN $\beta$  and ISG15 mRNAs.

### Discussion

Coronavirus DVGs are minigenomes derived from the coronavirus genome through recombination. In the present study, we dissected the function of individual DVGs at the level of their RNA structure, their encoded proteins and both in interferon signaling. We also showed that different DVGs have different effects on the synthesis of IFN $\beta$  and ISG15 mRNAs and the inhibition of

coronavirus replication either individually or collectively. In addition, because (i) the aim of this study was to examine the effects of DVGs on the synthesis of IFN $\beta$  and ISG15 mRNAs and coronavirus RNA and (ii) the measurement of IFN and ISGs at the mRNA level has been extensively employed for the study of innate immunity [37, 45, 46], (i) to be consistent and then to compare the synthesis efficiency of IFN $\beta$  and ISG15 mRNAs and coronavirus RNA on the same basis and (ii) to connect the alteration of IFN $\beta$  mRNA with that of downstream ISG15 mRNA and with subsequent coronavirus RNA synthesis, quantitation of IFN $\beta$  and ISG15 and coronavirus replication at the RNA level was performed. Thus, based on the results of the study, coronavirus RNA synthesis can be regulated by its genome-derived DVGs at least partly through the interferon signaling pathway in different infection settings. The biological relevance and potential antiviral applications derived from this study are discussed below.

The number of DVGs derived from SARS-CoV-2 is correlated with the level of host IFN response and disease development [26]. However, whether the induction of interferon signaling is due to the RNA structure of the DVG or DVG-encoded protein, or the combination of both remains to be clarified. Consequently, unlike previous studies, by specifically dissecting individual coronavirus DVG 2.2 and DVG 5.1 at the levels of RNA, protein and both in the present study, it is suggested that the DVG, DVG-encoded protein, and the combination of both can affect interferon signaling. In addition, the RNA structure and the encoded protein derived from the same individual DVG may have different effects on the induction of interferon signaling (for example, DVG 5.1, Fig. 3). Furthermore, previous studies have suggested that (i) coronaviruses can synthesize a variety of DVGs with different RNA structures (8); (ii) that coronavirus-DVGs can encode proteins [35]; and (iii) that RNA structures are correlated with the induction of innate immunity [19, 20]. Thus, the diversity of RNA structures, encoded proteins and combinations of both RNAs and proteins resulting from the diverse DVGs synthesized in coronavirus-infected cells may have various effects on coronavirus replication and cellular biological processes through different pathways, including innate immunity. Consequently, these characteristics of coronavirus DVGs derived from the previous and the present studies may explain why the DVGs with different genome structures selected in the present study have diverse effects on innate immunity and coronavirus replication.

Like other positive-strand RNA viruses, coronaviruses can produce a double-strand (ds) RNA genome via coronavirus RNA-dependent RNA polymerase (RdRp) [47–50]. With respect to the DVG, the DVG cannot replicate by itself in uninfected cells because the

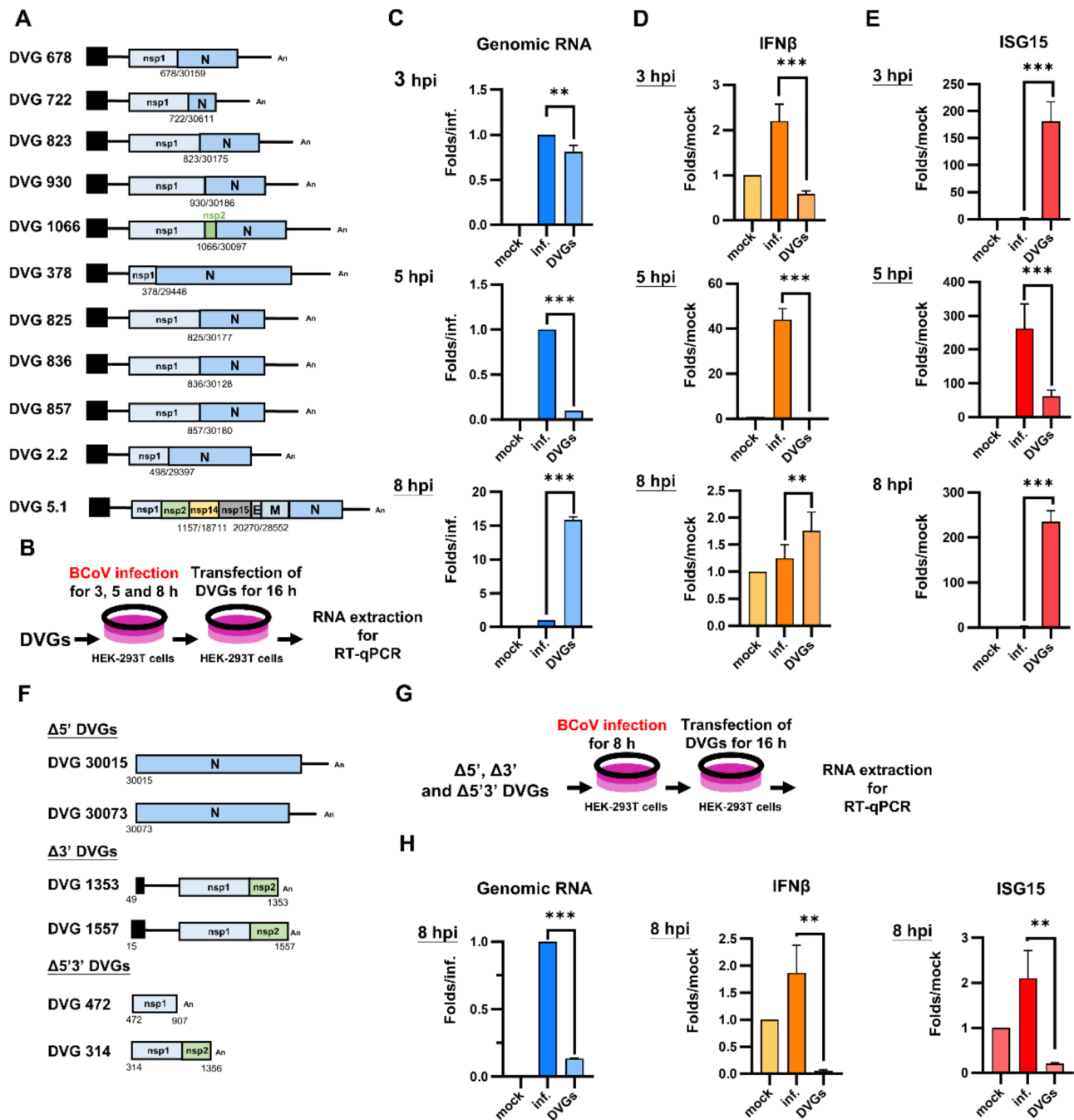


**Fig. 7** Coronavirus DVGs can collectively affect coronavirus RNA synthesis. **(A)** The genome structures of the naturally occurring BCoV DVGs selected in this experiment. The numbers below each DVG structure are the nucleotide positions at which recombination occurred. **(B)** Diagram depicting the experimental procedure used to examine the effects of the selected DVGs on BCoV RNA synthesis, in which the selected DVGs were transfected together in the same plate after BCoV infection. **(C)** Comparison of the relative amounts of BCoV RNA between mock-transfected and DVG-transfected HEK-293T cells that were first infected with BCoV and then transfected with DVGs at 3 (upper panel), 5 (middle panel) and 8 (lower panel) hpi. “Mock” indicates that the HEK-293T cells were mock-transfected and mock-infected. The “Folds/inf.” on the y-axis is presented as relative units of BCoV RNA compared with the amount of BCoV RNA in mock-transfected and BCoV-infected cells (the amount of BCoV RNA in mock-transfected and BCoV-infected cells (inf.) = 1). **(D)** and **(E)** Comparison of the relative expression of IFNβ mRNA **(D)** and ISG15 mRNA **(E)** between mock-transfected HEK-293T cells and DVG-transfected HEK-293T cells, which were first infected with BCoV and then transfected with DVG at 3, 5 and 8 hpi. The “Folds/mock” on the y-axis is presented as relative units of mRNA compared with the amount of mRNA in mock-transfected and mock-infected cells (the amount of mRNA in mock-transfected and mock-infected cells (mock) = 1). **(F)** The genome structures of the naturally occurring BCoV DVGs with missing 5' (Δ5' DVG) or 3' (Δ3' DVG) or both (Δ5'3' DVG) UTRs selected in this experiment. **(G)** Diagram depicting the experimental procedure used to examine the effects of the selected DVGs **(F)** on BCoV RNA synthesis, in which the selected DVGs were transfected together in the same plate after BCoV infection. **(H)** Effects of the DVGs shown in **(F)** collectively on coronavirus RNA synthesis (left panel) and interferon signaling (middle and right panels) in HEK-293T cells, which were first infected with BCoV and then transfected with DVGs at 8 hpi. \*\**p* < 0.01, \*\*\**p* < 0.001

DVG cannot encode RdRp due to the internal deletion of the DVG (compared with the full-length coronavirus genome). Consequently, to replicate [29], the coronavirus DVG needs to use its standard coronavirus-encoded RdRp in standard coronavirus-infected cells to produce the negative-strand DVG via the positive-strand DVG genome as a template, and the dsDVG, which consists of DVG and antiDVG hybrids (that is, the replicative form), can therefore be generated. Confirming the synthesis of the dsDVG would be interesting since a dsDVG can be synthesized. However, because (i) the dsDVG can be synthesized only in the presence of its standard coronavirus and (ii) both the full-length standard coronavirus dsRNA genome and dsDVG can be generated in standard coronavirus-infected cells, specifying which fluorescence signals are derived from the full-length standard coronavirus dsRNA genome and which signals are derived from the dsDVG is unlikely. Consequently, the identification of dsDVGs was not performed in this study. Nevertheless, on the basis of the results of the present study, it is speculated that (i) in uninfected cells, the synthesis of IFN $\beta$  and ISG15 mRNAs can be induced by the DVG RNA structure (Figs. 1, 3 and 5), and (ii) in BCoV-infected cells, the synthesis of IFN $\beta$  and ISG15 mRNAs can be induced by both the DVG RNA structure and dsDVG (Figs. 2, 4 and 6).

To confirm whether only the encoded protein itself is the sole factor impacting the synthesis of IFN $\beta$  and ISG15 mRNAs, the transfection of the DVG-containing plasmid instead of the *in vitro*-transcribed DVG was considered. However, as suggested above, the RNA structures of DVGs themselves, which are produced from plasmids via the cellular transcription machinery, are also likely to affect the synthesis of the IFN $\beta$  and ISG15 mRNAs. Consequently, both (i) the transcribed DVG and (ii) the encoded protein derived from the plasmid, but not the encoded protein itself derived from the plasmid, are factors affecting the synthesis of the IFN $\beta$  and ISG15 mRNAs. These experimental conditions actually resemble those in the current study shown in Figs. 1 and 3, in which DVGs 2.2 and 5.1 can also affect the synthesis of IFN $\beta$  and ISG15 mRNAs at both the RNA and protein levels. The only difference between the two experiments is that the generation of the DVG transcript is from *in vitro* transcription (Figs. 1 and 3) or from the cellular transcription machinery if a transfected plasmid is used. Therefore, such an experimental design based on plasmid transfection may not confirm that the encoded protein is the sole factor affecting the synthesis of IFN $\beta$  and ISG15 mRNAs.

To examine the effects of coronavirus-DVGs on coronavirus RNA synthesis under different infection conditions, DVGs were transfected into cells before or after coronavirus infection. The resulting strength of innate

immunity is highly correlated with that of inhibitory efficiency of coronavirus RNA synthesis in cells first transfected with DVGs followed by infection (Figs. 2B, 4B and 5E), suggesting that DVGs have the ability to inhibit coronavirus RNA synthesis through the induction of innate immunity. However, the correlation between the strength of DVG-induced innate immunity and the inhibitory efficiency of coronavirus RNA synthesis was not obvious in cells first infected with coronavirus and then transfected with DVG, as shown in Figs. 2D, 4D, 6 and 7. The reasons leading to the differences are explained as follows. In cells first infected with coronavirus followed by DVG transfection, coronavirus–host interactions are initiated before the transfection of DVGs. During coronavirus–host interactions, the cell defense system is activated, and coronavirus also triggers its inhibitory effects to counteract cellular defenses. The altered cell environment caused by virus–host interactions may subsequently affect the functions of the transfected DVGs at the RNA, protein and combined levels, resulting in altered biological processes, including DVG-induced interferon signaling. Consequently, in addition to various levels of innate immunity, other biological processes or pathways may also affect coronavirus RNA synthesis. Thus, there is no obvious correlation between the strength of DVG-induced innate immunity and the inhibitory efficiency of coronavirus RNA synthesis in cells first infected with coronavirus and then transfected with DVGs. Accordingly, when DVG 5.1 is used as an example, in cells first transfected with DVGs followed by infection, DVG 5.1 can induce interferon signaling. Thus, it is reasonable to conclude that the innate immunity previously activated by the transfection of DVG 5.1 is the main factor leading to the inhibition of coronavirus RNA synthesis. However, in cells first infected with coronavirus and then transfected with DVG 5.1, DVG 5.1 may not have the same ability to induce interferon signaling because coronavirus–host interactions alter the infection environment and subsequent biological processes. Thus, the altered biological processes may affect the induction strength of interferon signaling derived from DVG 5.1 at the RNA, protein or combined levels. In line with this, because (i) the assembly of viral particles is related to the viral titer and (ii), as mentioned above, the altered cell environment caused by virus–host interactions and the functions of the transfected DVGs may also alter cellular biological processes and thus the efficiency of virus assembly, the altered levels of coronavirus RNA synthesis may therefore not always be closely related to those of coronavirus titers (Figs. 2, 4, 5, 6 and 7 and S7–S11). Consequently, in addition to innate immunity, other factors derived from altered biological processes may also affect the efficiency of coronavirus RNA synthesis and titers, leading to no obvious correlation (i) between innate immunity and the

inhibitory efficiency of coronavirus RNA synthesis and (ii) between virus titer and coronavirus RNA synthesis in the infection cells transfected with DVGs. Notably, the different strengths of the induction of innate immunity and the inhibition of coronavirus RNA synthesis in DVG-transfected cells before or after infection may also indicate that DVGs may have different regulatory functions in coronavirus RNA synthesis at different stages of infection.

Furthermore, the coronavirus DVG is also called a defective interfering (DI) RNA because, similar to the DI RNAs of other RNA viruses, it has been postulated to interfere with the replication of its parental (standard) virus by competing with replication resources [1, 51, 52]. On the basis of the data shown in Figs. S1–S6, the DVGs have the potential to replicate in the presence of standard BCoV; thus, DVGs with greater replication efficiency may compete with the standard virus BCoV for replication resources, leading to a reduced level of BCoV replication. Consequently, because the DVGs selected in this study can all induce the synthesis of IFN $\beta$  and ISG15 mRNAs (Fig. 6), it is speculated that, in addition to innate immunity, the inhibitory effect of DVGs on BCoV replication shown in this study may also result from the competition of replication resources between DVGs and the BCoV standard virus.

Previous studies have shown that DVG species can be altered under different infection environments [8] and undergo mutations under the selection pressures of antivirals and persistent infection [53]. Since (i) coronavirus DVG species can be altered under different infection environments [8], (ii) coronavirus DVGs have diverse effects on innate immunity (Fig. 5C), and (iii) DVGs have different effects on coronavirus RNA synthesis (Fig. 5E), it is proposed that, under altered infection environments, coronaviruses may synthesize different DVGs to regulate virus–host interactions, such as innate immunity and coronavirus RNA synthesis, altering coronavirus–host interactions to enhance the survival of coronaviruses. Consequently, in addition to the regular infection environment, coronaviruses may also regulate coronavirus RNA synthesis and subsequent protein synthesis via their DVGs to optimize their infection in altered infection environments. Such regulation between the coronavirus genome and coronavirus DVGs may therefore affect pathogenesis and increase the complexity of controlling the virus. Additionally, such characteristics may benefit the survival of coronaviruses because the regulation of coronavirus RNA synthesis by DVGs may halt the adverse effects on cell integrity, and thus coronaviruses can replicate in cells for a longer time to produce more virus progeny. This finding also supports and explains the previous results in which persistent infection with paramyxovirus was correlated with DVGs [54].

The aim of this study was to examine whether different coronavirus DVGs with different RNA structures can induce different levels of IFN- $\beta$  mRNA and downstream ISG15 mRNA and thus affect coronavirus replication via the transfection of in vitro-synthesized DVGs. Consequently, cells (i) with a high transfection efficiency, (ii) in which the IFN response can be triggered by in vitro-synthesized DVGs and (iii) that are permissive to BCoV infection are considered. Because (i) HEK-293T cells have a high transfection efficiency [36], (ii) BCoV can replicate in HEK-293T cells and (iii) IFN $\beta$  and downstream ISG15 mRNAs can also be induced in HEK-293T cells [37, 38], HEK-293T cells and BCoV are selected for this study. Although HEK-293T cells are not primary cells, the IFN response can still be activated through detection of the viral RNA structure in the cytoplasm, as indicated by the results derived from previous studies [37, 38, 45, 46, 55] and our current results (Figs. 1, 2, 3, 4, 5, 6 and 7), in which the IFN $\beta$  mRNA and downstream ISG mRNA can be induced in HEK-293 and HEK-293T cells. Consequently, although the current study is not performed in a physiologically relevant setting for BCoV and has the aforementioned limitations, the current results still can support the aim of the study that different DVGs can lead to different synthesis efficiencies of IFN $\beta$  and downstream ISG15 mRNAs and affect coronavirus replication via the transfection of in vitro-synthesized DVGs in HEK-293T cells.

Thus, the findings of the present study suggest that coronavirus DVGs can induce innate immunity and inhibit coronavirus replication with different strengths at the level of RNA or protein or both, either individually or collectively. The diverse RNA structures and encoded proteins resulting from diverse DVG populations synthesized in coronavirus-infected cells can lead to diverse effects on coronavirus–host interactions, including different levels of activation in innate immunity and inhibition of coronavirus replication. These diverse effects caused by coronavirus DVGs may regulate coronavirus replication and overcome adverse environments, contributing to the survival and pathogenesis of this disease. Thus, in addition to its role in innate immunity, DVGs may also exert their functions via their RNA structure or encoded protein to affect coronavirus–host interactions through other biological pathways. On the other hand, since DVGs have the ability to inhibit coronavirus RNA synthesis at the level of RNA, protein or both, it is argued that the DVG populations in infected cells are resources for the identification of antivirals. Consequently, the experimental system used in the present study can be used as a platform to identify antivirals from DVG populations on the basis of their RNA structures, encoded proteins or both.

## Conclusions

In the present study, by dissecting the function of individual DVGs, it is suggested that DVGs have different effects on interferon signaling at the level of RNA, encoded proteins or both. In addition, different DVGs have different effects on the induction of interferon signaling and the inhibition of coronavirus replication both individually and collectively under different infection conditions. Thus, coronavirus replication can be regulated by coronavirus genome-derived DVGs. Such regulation between the coronavirus genome and coronavirus DVGs may enhance the survival of coronavirus and therefore is correlated to pathogenesis. Lastly, because DVGs can induce innate immunity at the level of RNA, protein or both and coronavirus RNA synthesis can be inhibited by DVGs at least through induction of innate immunity, the diverse DVG populations in infected cells are resources for the identification of antivirals, and the methods used in the current study can be used as a platform for this purpose.

## Abbreviations

BCoV	Bovine coronavirus
UTR	Untranslated region
ORF	Open reading frame
MDA5	Melanoma differentiation-associated gene 5
RIG-I	Retinoic acid-inducible gene 1
HA	Hemagglutination
HEK-293T	Human embryonic kidney 293T
IFN	Interferon
ISG	IFN-stimulated gene
DMEM	Dulbecco's modified Eagle's medium

## Supplementary Information

The online version contains supplementary material available at <https://doi.org/10.1186/s12985-025-02654-5>.

Supplementary Material 1

## Acknowledgements

We thank Dr. David A. Brian at University of Tennessee, Knoxville, for providing BCoV.

## Author contributions

Conceptualization: HWH, LKC and HYW; Methodology: HWH, LKC, CCY, CHL, YT, PCH, CYY and HYW; Investigation: HWH, LKC and HYW; Resources: HYW; Writing—Original Draft: HWH and HYW; Writing—Review and Editing: HWH and HYW; Supervision: HYW; Funding Acquisition: HYW.

## Funding

This work was supported by grant 113-2313-B-005-009-MY3 from National Science and Technology Council, Taiwan.

## Data availability

No datasets were generated or analysed during the current study.

## Declarations

### Ethics approval and consent to participate

Not applicable.

### Consent for publication

Not applicable.

## Competing interests

The authors declare no competing interests.

Received: 11 November 2024 / Accepted: 6 February 2025

Published online: 14 February 2025

## References

1. Brian DA, Baric RS. Coronavirus genome structure and replication. *Curr Top Microbiol Immunol*. 2005;287:1–30.
2. Gorbalenya AE, Enjuanes L, Ziebuhr J, Snijder EJ. Nidovirales: evolving the largest RNA virus genome. *Virus Res*. 2006;117(1):17–37.
3. Xiao SY, Wu YJ, Liu H. Evolving status of the 2019 novel coronavirus infection: proposal of conventional serologic assays for disease diagnosis and infection monitoring. *J Med Virol*. 2020;92(5):464–7.
4. Yang WJ, Cao QQ, Qin L, Wang XY, Cheng ZH, Pan AS, et al. Clinical characteristics and imaging manifestations of the 2019 novel coronavirus disease (COVID-19): a multi-center study in Wenzhou city, Zhejiang, China. *J Infect*. 2020;80(4):388–93.
5. Zaki AM, van Boheemen S, Bestebroer TM, Osterhaus AD, Fouchier RA. Isolation of a novel coronavirus from a man with pneumonia in Saudi Arabia. *N Engl J Med*. 2012;367(19):1814–20.
6. Decaro N, Mari V, Desario C, Campolo M, Elia G, Martella V, et al. Severe outbreak of bovine coronavirus infection in dairy cattle during the warmer season. *Vet Microbiol*. 2008;126(1–3):30–9.
7. V'kovski P, Kratzel A, Steiner S, Stalder H, Thiel V. Coronavirus biology and replication: implications for SARS-CoV-2. *Nat Rev Microbiol*. 2021;19(3):155–70.
8. Lin CH, Chen B, Chao DY, Hsieh FC, Yang CC, Hsu HW, et al. Unveiling the biology of defective viral genomes in vitro and in vivo: implications for gene expression and pathogenesis of coronavirus. *Viol J*. 2023;20(1):225.
9. Kim D, Lee JY, Yang JS, Kim JW, Kim VN, Chang H. The Architecture of SARS-CoV-2 Transcriptome. *Cell*. 2020;181(4):914–.
10. Vignuzzi M, López CB. Defective viral genomes are key drivers of the virus–host interaction. *Nat Microbiol*. 2019;4(7):1075–87.
11. Brian DA, Spaan WJM. Recombination and coronavirus defective interfering RNAs. *Semin Virol*. 1997;8(2):101–11.
12. Baum A, Sachidanandam R, García-Sastre A. Preference of RIG-I for short viral RNA molecules in infected cells revealed by next-generation sequencing (107, pg 16303, 2010). *P Natl Acad Sci USA*. 2011;108(7):3092.
13. Li Y, Renner DM, Comar CE, Whelan JN, Reyes HM, Cardenas-Diaz FL, et al. SARS-CoV-2 induces double-stranded RNA-mediated innate immune responses in respiratory epithelial-derived cells and cardiomyocytes (118, e2022643118, 2021). *P Natl Acad Sci USA*. 2023;120:29.
14. Kikkert M. Innate Immune Evasion by Human respiratory RNA viruses. *J Innate Immun*. 2020;12(1):4–20.
15. Yoneyama M, Kikuchi M, Natsukawa T, Shinobu N, Imaizumi T, Miyagishi M, et al. The RNA helicase RIG-I has an essential function in double-stranded RNA-induced innate antiviral responses. *Nat Immunol*. 2004;5(7):730–7.
16. Andrejeva J, Childs KS, Young DF, Carlos TS, Stock N, Goodbourn S et al. The V proteins of paramyxoviruses bind the IFN-inducible RNA helicase, mda-5, and inhibit its activation of the promoter. *P Natl Acad Sci USA*. 2004;101(49):17264–9.
17. Pichlmair A, Schulz O, Tan CP, Näslund TI, Liljeström P, Weber F, et al. RIG-I-mediated antiviral responses to single-stranded RNA bearing 5'-phosphates. *Science*. 2006;314(5801):997–1001.
18. Hornung V, Ellegast J, Kim S, Brzózka K, Jung A, Kato H, et al. 5'-triphosphate RNA is the ligand for RIG-I. *Science*. 2006;314(5801):994–7.
19. Gitlin L, Barchet W, Gilfillan S, Cella M, Beutler B, Flavell RA, et al. Essential role of mda-5 in type I IFN responses to polyriboinosinic: polyribocytidylic acid and encephalomyocarditis picornavirus. *P Natl Acad Sci USA*. 2006;103(22):8459–64.
20. Kato H, Takeuchi O, Sato S, Yoneyama M, Yamamoto M, Matsui K, et al. Differential roles of MDA5 and RIG-I helicases in the recognition of RNA viruses. *Nature*. 2006;441(7089):101–5.
21. Pichlmair A, Schulz O, Tan CP, Rehwinkel J, Kato H, Takeuchi O, et al. Activation of MDA5 requires higher-order RNA structures generated during virus infection. *J Virol*. 2009;83(20):10761–9.
22. Witteveldt J, Blundell R, Maarleveld JJ, McFadden N, Evans DJ, Simmonds P. The influence of viral RNA secondary structure on interactions with innate host cell defences. *Nucleic Acids Res*. 2014;42(5):3314–29.

23. Stark GR, Kerr IM, Williams BRG, Silverman RH, Schreiber RD. How cells respond to interferons. *Annu Rev Biochem.* 1998;67:227–64.
24. Takaoka A, Yanai H. Interferon signalling network in innate defence. *Cell Microbiol.* 2006;8(6):907–22.
25. Ortega-Prieto A, Jimenez-Guardeño JM. Interferon-stimulated genes and their antiviral activity against SARS-CoV-2. *Mbio.* 2024.
26. Zhou TRY, Gilliam NJ, Li SZ, Spandau S, Osborn RM, Connor S et al. Generation and Functional Analysis of defective viral genomes during SARS-CoV-2 infection. *Mbio.* 2023;14(3).
27. Girgis S, Xu ZK, Oikonomopoulos S, Fedorova AD, Tchesnokov EP, Gordon CJ et al. Evolution of naturally arising SARS-CoV-2 defective interfering particles. *Commun Biol.* 2022;5(1).
28. Lin CH, Chen B, Chao DY, Hsieh FC, Lai CC, Wang WC, et al. Biological characterization of coronavirus noncanonical transcripts in vitro and in vivo. *Viol J.* 2023;20(1):232.
29. Chang RY, Hofmann MA, Sethna PB, Brian DA. A cis-acting function for the coronavirus leader in defective interfering RNA replication. *J Virol.* 1994;68(12):8223–31.
30. Lin CH, Hsieh FC, Chang YC, Yang CY, Hsu HW, Yang CC, et al. Targeting the conserved coronavirus octamer motif GGAAGAGC is a strategy for the development of coronavirus vaccine. *Viol J.* 2023;20(1):267.
31. Sato K, Inaba Y, Kurogi H, Takahashi E, Satoda K, Omori T, et al. Hemagglutination by Calf Diarrhea Coronavirus. *Vet Microbiol.* 1977;2(1):83–7.
32. Zhang YF, Han L, Xia L, Yuan YX, Hu H. Assessment of hemagglutination activity of porcine. *J Vet Sci.* 2020;21(1).
33. Strahle L, Garcin D, Kolakofsky D. Sendai virus defective-interfering genomes and the activation of interferon-beta. *Virology.* 2006;351(1):101–11.
34. Vignuzzi M, Lopez CB. Defective viral genomes are key drivers of the virus-host interaction. *Nat Microbiol.* 2019;4(7):1075–87.
35. Lin CH, Hsieh FC, Lai CC, Wang WC, Kuo CY, Yang CC, et al. Identification of the protein coding capability of coronavirus defective viral genomes by mass spectrometry. *Viol J.* 2023;20(1):290.
36. Warga E, Anderson J, Tucker M, Harris E, Elmer J. Transcriptomic analysis of the innate immune response to in vitro transfection of plasmid DNA. *Mol Ther Nucleic Acids.* 2023;31:43–56.
37. Zhang XB, Yuan ZF, Geng JJ, Gong ZAD, Wei SC. Bovine coronavirus nucleocapsid suppresses IFN- $\beta$  production by inhibiting RIG-I-like receptors pathway in host cells. *Arch Microbiol.* 2022;204(8).
38. Ferreira CB, Sumner RP, Rodriguez-Plata MT, Rasaiyaah J, Milne RS, Thrasher AJ, et al. Lentiviral Vector Production Titer is not limited in HEK293T by Induced Intracellular Innate Immunity. *Mol Ther Methods Clin Dev.* 2020;17:209–19.
39. Lo CY, Tsai TL, Lin CN, Lin CH, Wu HY. Interaction of coronavirus nucleocapsid protein with the 5'- and 3'-ends of the coronavirus genome is involved in genome circularization and negative-strand RNA synthesis. *FEBS J.* 2019;286(16):3222–39.
40. Tsai TL, Lin CH, Lin CN, Lo CY, Wu HY. Interplay between the poly(A) tail, poly(A)-Binding protein, and Coronavirus Nucleocapsid protein regulates Gene expression of Coronavirus and the host cell. *J Virol.* 2018;92(23).
41. Williams GD, Chang RY, Brian DA. A phylogenetically conserved hairpin-type 3' untranslated region pseudoknot functions in coronavirus RNA replication. *J Virol.* 1999;73(10):8349–55.
42. Wu HY, Brian DA. 5'-proximal hot spot for an inducible positive-to-negative-strand template switch by coronavirus RNA-dependent RNA polymerase. *J Virol.* 2007;81(7):3206–15.
43. Wu HY, Brian DA. Subgenomic messenger RNA amplification in coronaviruses. *Proc Natl Acad Sci U S A.* 2010;107(27):12257–62.
44. Wu HY, Ozdarendeli A, Brian DA. Bovine coronavirus 5'-proximal genomic acceptor hotspot for discontinuous transcription is 65 nucleotides wide. *J Virol.* 2006;80(5):2183–93.
45. AIDaif BA, Mercer AA, Fleming SB. The parapoxvirus Orf virus inhibits IFN- $\beta$  expression induced by dsRNA. *Virus Res.* 2022;307.
46. Wienert B, Shin J, Zelin E, Pestal K, Corn JE. In vitro-transcribed guide RNAs trigger an innate immune response via the RIG-I pathway. *PLoS Biol.* 2018;16(7).
47. Feng Q, Hato SV, Langereis MA, Zoll J, Virgen-Slane R, Peisley A, et al. MDA5 detects the double-stranded RNA replicative form in picornavirus-infected cells. *Cell Rep.* 2012;2(5):1187–96.
48. Triantafyllou K, Vakakis E, Kar S, Richer E, Evans GL, Triantafyllou M. Visualisation of direct interaction of MDA5 and the dsRNA replicative intermediate form of positive strand RNA viruses. *J Cell Sci.* 2012;125(Pt 20):4761–9.
49. Weber F, Wagner V, Rasmussen SB, Hartmann R, Paludan SR. Double-stranded RNA is produced by positive-strand RNA viruses and DNA viruses but not in detectable amounts by negative-strand RNA viruses. *J Virol.* 2006;80(10):5059–64.
50. Chen YG, Hur S. Cellular origins of dsRNA, their recognition and consequences. *Nat Rev Mol Cell Bio.* 2022;23(4):286–301.
51. Barrett AD, Dimmock NJ. Defective interfering viruses and infections of animals. *Curr Top Microbiol Immunol.* 1986;128:55–84.
52. Perrault J. Origin and replication of defective interfering particles. *Curr Top Microbiol Immunol.* 1981;93:151–207.
53. Lin CH, Tam HM, Yang CY, Hsieh FC, Wang JL, Yang CC et al. Evolution of the coronavirus spike protein in the full-length genome and defective viral genome under diverse selection pressures. *J Gen Virol.* 2023;104(11).
54. Xu J, Sun Y, Li Y, Ruthel G, Weiss SR, Raj A, et al. Replication defective viral genomes exploit a cellular pro-survival mechanism to establish paramyxovirus persistence. *Nat Commun.* 2017;8(1):799.
55. Edalat F, Khakpour N, Heli H, Letafati A, Ramezani A, Hosseini SY, et al. Immunological mechanisms of the nucleocapsid protein in COVID-19. *Sci Rep.* 2024;14(1):3711.

## Publisher's note

Springer Nature remains neutral with regard to jurisdictional claims in published maps and institutional affiliations.